Received: 25 October 2017 | Revised: 17 April 2018 | Accepted: 1 July 2018

DOI: 10.1002/pat.4410

RESEARCH ARTICLE

WILEY polymers advanced technologies

Formulation of micro-phase separation kinetics of polyurethane nanocomposites

Iman Sahebi Jouibari | Vahid Haddadi-Asl | Mohammad Masoud Mirhosseini

Department of Polymer Engineering and Color Technology, Amirkabir University of Technology (Tehran Polytechnic), Tehran, Iran

Correspondence
Vahid Haddadi-Asl, Department of Polymer Engineering and Color Technology, Amirkabir University of Technology (Tehran Polytechnic), Tehran, Iran.
Email: haddadi@aut.ac.ir

In the present study, thermoplastic polyurethane elastomers (TPUs) reinforced with multi-walled carbon nanotubes, Closite 30B nanoplates, and halloysite nanotubes were produced via melt compounding approach and evaluated with many techniques including microscopy, spectroscopy, thermal, and rheological analyses. Following primary analyses, time sweep tests were used to determine the influence of temperature, applied preshear, and type of nanofillers on the micro-phase separation kinetics of the nanocomposites. Based on the experimental results, a semi-experimental equation was developed to explain the relation between those parameters and micro-phase separation time. The equation is able to predict micro-phase separation time of TPU nanocomposites possessing different nanofillers at various shear rates and temperatures.

KEYWORDS

micro-phase separation, nanofillers, polyurethane, rheology, shear rate

1 | INTRODUCTION

Polyurethanes (PUs), amongst the most important engineering polymers, have been extensively used in many applications as diverse as adhesives, flexible or rigid foams, coating, fibers, elastomers, etc. PU can be formed by a simple step-growth polymerization reaction between isocyanate and diol groups. Different types of raw materials are used to produce PUs, and it is possible to tailor final properties of the products based on selection of these ingredients.[1-5] Thermoplastic polyurethane elastomers (TPUs) are amongst the most eminent classes of PUs composed of high *glass transition temperature* (T_g) or high melting temperature (T_m) hard segments and relatively low T_g soft segments covalently connected together. Thermodynamic incompatibility of soft and hard segments at low temperature results in a micro-phase separated domain structure.[6-9]

When the temperature reduces below the T_m of the crystalline segment of a block copolymer, concurrent phase separation and crystallization are foreseen. From a thermodynamic standpoint, phase separation precedes crystallization; however, both of which affect the final morphology and properties of the polymers.[10,11]

Many factors like polymerization methods, chemical structure of the hard and soft segments, process parameters (melting rate, cooling rate, solvent evaporation rate, shear rate, temperature, etc), and the presence of nanofillers affect the morphology and micro-phase separation of the PU elastomers.[12,13]

When the effect of nanofillers is studied on the micro-phase separated structure of TPU nanocomposites, physiochemical characteristics of the nanofillers like particle size, aspect ratio, shape, chemical nature, surface charge, and their interaction with polymer chains should be taken account.[14-16] For instances, Barick and Tripathy have shown that the incorporation of the multi-walled carbon nanotubes (MWCNTs) in TPU matrix not only accelerates the micro-phase separation structures of the TPU matrix but also changes the molecular weights of the soft and hard segments.[17] Moreover, the crystallinity of the TPU/MWCNT nanocomposites has been noticeably increased comparing pristine TPU due to positive nucleating effect of MWCNTs. Gupta et al have reported that incorporation of the MWCNTs into the PU matrix increases the onset and peak temperatures of crystallization, whereas decreases the activation energy of the nanocomposites due to heterogeneous nucleation effect of the MWCNTs.[18] Song et al have proposed that the incorporation of clay nanoplates into the PU matrix decreases the size of the spherical aggregates, corroborating the key role of clay nanoplates on the aggregation performance of the hard domains.[19]

Unlike the low molecular weight materials, polymers are very sensitive to flow field (shear or elongational forces) in their phase

separation performances. It is well understood that applying a shear before and/or during the semicrystalline polymer crystallization alters its subsequent morphology. Effect of flow field on the micro-phase separation and crystallization of the PUs has been the subject of few studies in literatures.[20] For example, nano-structuring kinetics of thermoplastic segmented PUs with or without preshear has been studied by Mourier et al.[21,22] It has been reported that the sensitivity of the structuring kinetics to the shear treatment is highly reliant on the composition and molar mass of the PUs. Moreover, a shear treatment applied at the beginning of the structuring appreciably reduces the structuring time. Consequently, the shear flow is found to decrease the entropy of the polymer chains and make them be aligned, thus promoting the kinetics of crystallization. On the other hand, in the presence of nanofillers, chain dynamics decrease in order to trap the chains onto the nanofiller surfaces and prevent chain orientation. Collectively, the shear flow and nanofillers simultaneously affect the micro-phase separation and crystallization of the PUs.[23-25] Considering the indispensable role of shear force and nanofillers in both laboratory and industrial processes (extrusion, injection moulding, etc) of PU, it would be imperative to study the effect of the aforesaid parameters on the micro-phase separation of the PUs. Hence, the goal of this work was to investigate the effect of temperature, preshear, and nanofillers with different aspect ratios and structures (MWCNTs, Closite 30B nanoplates [CBNPs], and halloysite nanotubes [HNTs]) on the micro-phase separation of TPU nanocomposites. To this end, firstly, TPUs based on poly(tetramethylene ether) glycol (PTMG), 4,4′-diphenylmethane diisocyanate (MDI), and 1,4-butanediol (BDO) were synthesized. Thereafter, TPU nanocomposites were prepared by melt processing and evaluated by many techniques including Fourier transform infrared (FTIR) spectroscopy, scanning electron microscopy (SEM), atomic force microscopy (AFM), dynamic mechanical-thermal analysis (DMTA), differential scanning calorimetry (DSC) thermograms, and rheometric mechanical spectrometer.

2 | MATERIALS AND METHODS

2.1 | Materials

Poly(tetramethylene ether) glycol (PTMG) with functionality of 2 and number–average molecular weight of 2000 (gr/gmol), MDI, BDO, and HNTs with inner diameter of 30 to 70 nm, pore volume of 1.26 to 1.34 mL/g, and specific surface of 64 m^2/g were purchased from Sigma-Aldrich. Organiclay modified clay Closite 30B (CEC: 90 meq/100 g) were obtained from southern Clay product. The multi-wall carbon nanotubes, Nanocyl 7000, with average diameter of 9.5 nm, average length of 1.5 μm, and purity of 90% supplied by Nanocyl (Belgium). *N,N*-Dimethylacetamide was obtained from Merck. All reagents were used as received without any further purification.

2.2 | Synthesis of TPU

TPU was synthesized by two-step solution polymerization method. Polymerization was carried out into a two-necked round-bottomed flask equipped with a vacuum inlet tube and a raw material entrance. The reaction assembly was placed in a heating oil bath. Prior to mixing, PTMG, MDI, and BDO were dried in a vacuum oven at 80°C for 3 hours to ensure residual moisture removal. For PU synthesis, the molar ratio of PTMG, MDI, and BDO were determined to be 1, 3, and 2, respectively. Thirty-gram PTMG with 45-mL *N,N*-dimethylacetamide was added to the flask. Later on, 11.6-g MDI was added to the content and reacted with polyol for 3 hours at 75 to 85°C under continuous stirring to render a macro diisocyanate prepolymer. In the chain extension step, 2.74-g BDO was added to the prepolymer. During this step, the viscosity of PU slowly increased due to the ongoing chain-extension reaction. After 3-hour reaction, the viscous liquid obtained was poured into a silicone mold and placed in an oven at 85°C for 24 hours. Finally, all samples were removed from the mold and stored at ambient temperature.

2.3 | TPU nanocomposites preparation

Nanocomposites were prepared via melt compounding method. To this end, TPU and varying content of CBNPs, HNTs, and MWNTs (gamut from 0.1 to 5%wt) were compounded with a laboratory internal mixer (Braebender Plasticorder W50). Processing parameters, ie, temperature and rotating speed were optimized as 210°C and 100 rpm, respectively. Melt-compounding was carried on for 18 minutes for nanocomposite comprising the CBNPs and 15 minutes for nanocomposites containing the MWNTs and HNTs. Prior to mixing; TPUs were dried in a vacuum oven at 140°C for 12 hours to ensure residual moisture removal.

2.4 | Characterization

Fourier transform infrared (FTIR) spectra were recorded on a Bruker spectrophotometer in the range between 4400 and 500 cm^{-1}, with a resolution of 4 cm^{-1}.

Morphology of the samples was evaluated via field emission scanning electron microscopy (FESEM; Hitachi S4160) at an accelerating voltage of 30 kV after being sputter coated with Au particles.

Atomic force microscopy (AFM) was performed with a Dualscope/Rasterscope C26 (DME, Denmark) equipment in tapping mode on the thin film samples at room temperature. AFM images were processed using data processing software.

The thermal analysis of the samples was carried out on a differential scanning calorimeter (Flash DSC; Mettler-Toledo) with a temperature range of −50°C to 210°C and heating rate of 10°C/min under nitrogen atmosphere.

Dynamic mechanical properties of the nanocomposites were measured using dynamic mechanical thermal analyzer (Diamond DMA; Perkin Elmer) in the tensile mode, heating rate of 5°C/min, frequency of 1 Hz, and static force of 0.1 N on the molded samples (20 × 11 × 1 mm). The temperature dependence of the storage modulus (G′) and loss modulus (G″) was plotted in the range of −100°C to 150°C.

Rheometrics mechanical spectrometer (Paar Physica UDS200) equipped with a parallel plate fixture (diameter = 25 mm, constant gap = 1 mm) was used to measure the linear viscoelastic responses of the neat TPU and the nanocomposites and to assess the effects of nanofiller and pre-shear on the rheological responses. The neat

TPU was heated for 15 minutes and the nanocomposites for 5 minutes to remove thermal and processing history. Following heating, the samples were quickly cooled to annealing temperature (T_{ann}). Then, the storage modulus and the loss modulus of the samples at T_{ann} were measured by time sweep experiment for 2 hours to study the micro-phase separation and the hard domain aggregation. In order to assess the effect of shear flow on the phase separation kinetics, the time sweep experiment was performed at various preshear ranging from 5 to 30 1/s prior to time sweep test at annealing temperature. To discern micro-phase separation temperature, the cooling process was carried out at a rate of 10°C/min for neat the TPU and from melting temperature (210°C) to near the hard segments T_g (120°C) for the nanocomposites.

3 | RESULTS AND DISCUSSION

In systems containing two or more types of materials, the FTIR technique is an effective method to analyze functional groups. The FTIR spectra of the neat TPU and TPU nanocomposites are shown in Figure 1. The band at 1712 cm^{-1} can be assigned to H-bonded urethane carbonyl groups. The peaks at 2850 and 2930 cm^{-1} correspond to symmetric and non-symmetric stretching vibration of CH_2, respectively. The absorption band at 3320 cm^{-1} belongs to NH stretching.[26] As evidenced by Figure 1, the intensity of the hydrogen bonding related peak (at 1712 cm^{-1}) increases once HNTs and MWCNTs are added to TPU. The increment is more profound in the case of MWCNTs/TPU nanocomposites. However, when the CBNPs are added to the TPU, the peak intensity remains unchanged.

FESEM was employed to study the morphology and size of micro-phase separated domains. FESEM images of the neat TPU, TPU/CBNPs, TPU/HNTs, and TPU/MWCNTs are presented in Figure 2. TPU reveals cylindrical domains assigned to micro-phase separation

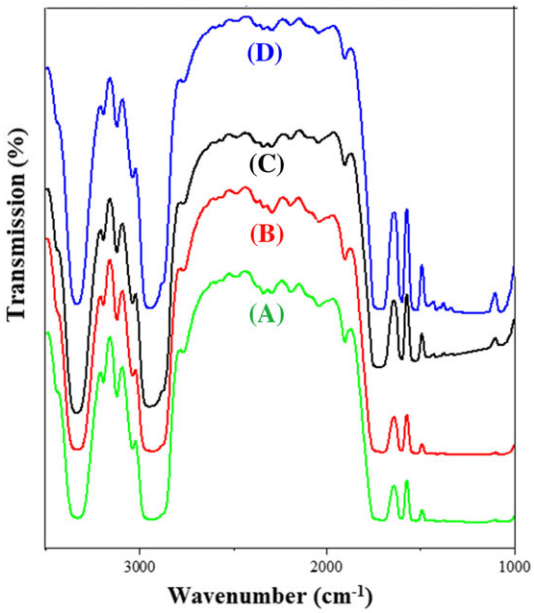

FIGURE 1 FTIR spectra of (A) neat TPU, (B) TPU/CBNPs, (C) TPU/HNTs, and (D) TPU/MWCNTs. Nanofiller content = 0.1 wt% [Colour figure can be viewed at wileyonlinelibrary.com]

of the hard and soft segments (Figure 2A). It is well known that the difference in chemical nature of the nanofillers leads to various interactions with PU chains. The MWCNTs and HNTs have more affinity to interact with hard segments than soft ones. The affinity is higher in case of MWCNTs. On the other hand, the CBNPs have propensity to interact with the soft segments. The presence of the CBNPs is evidenced from Figure 2B; while, micro-phase separated domains located on the MWCNTs are displayed in Figure 2D. The presence of micro-phase separated domains near the nanofillers corroborates the good affinity of the nanofillers to hard segments. Indeed, MWCNTs can act as effective nucleating agents to crystallize the TPU hard segments.

To assess whether the presence of nanofillers would affect the topology of the polymer nanocomposites, nanocomposite surfaces were analyzed by AFM. Depending on the chemical nature, the aspect ratio of the nanofillers and the nature of polymer carrying them, different changes in roughness are probable.[27] Figure 3 presents the AFM images of the neat TPU and the TPU nanocomposites. Because the soft segment can simply move, it was defined as a continuous phase embedding hard segment. Surface roughness of the neat TPU observed in Figure 3A can be assigned to micro-phase separation of the TPU caused by thermodynamic incompatibility between polar hard segments and much less polar soft segments. Once the MWCNTs are incorporated into TPU matrix, surface roughness decreases by 36.5% comparing the neat TPU. MWCNTs possess the high affinity to the hard segments and may conceal most of the hard segments into the PU bulk, thus decreasing the surface roughness. The CBNPs are not prone to the hard segments, thus are embedded in the soft segments and increase the roughness value from 159 nm (neat TPU) to 215 nm for the CBNP laden nanocomposite. The HNTs tend to interact with the hard segment but much lower than the MWCNTs. Accordingly, the average surface roughness of HNTs loaded nanocomposite decreases 8.8% compared with the neat one.

Based on the DMTA and DSC analyses, transition temperatures of the samples are discerned, and data are summarized in Table 1. In MWCNTs and HNTs loaded nanocomposites, nanofillers possess more tendencies to the hard segments; thus, the soft segments have more freedom to move. Hence, these composites have lower soft segment T_g comparing the ones with CBNPs. CBNPs have no affinity to the hard segments. They are embedded into the soft segments and prevent their mobility. Therefore, the presence of the CBNPs increases the T_g of the soft phase. The MWCNTs and HNTs raise the glass transition temperature of the hard phase. In the presence of MWCNTs, the crystallization temperature is substantially increased due to the outstanding ability of the MWCNTs to absorb hard segments and to act as nucleating agents.[28]

Because different factors like temperature, nanofillers, and shear flow affect the degree of micro-phase separation and crystallization of the PUs, attempts have been made to present a mathematical relation describing the role of said parameters on the micro-phase separation process. Rheology is a trustworthy method deducing the morphological feature of the complex fluids. The collision of storage and loss moduli as a function of time is a critical point of the physical gel (cross time).[29] The storage and loss moduli of the samples as a function of time at 150°C are shown in Figure 4. As evidenced from the

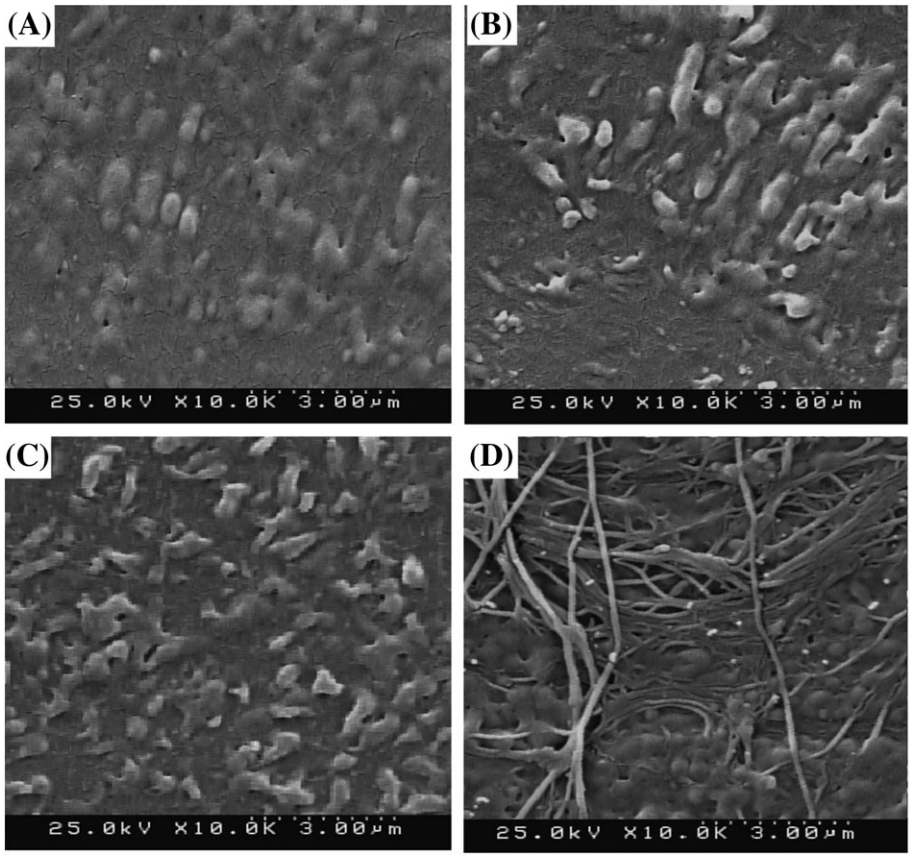

FIGURE 2 FESEM images of samples (A) neat TPU, (B) TPU/CBNPs, (C) TPU/HNTs, and (D) TPU/MWCNTs. Nanofiller content = 0.1 wt%

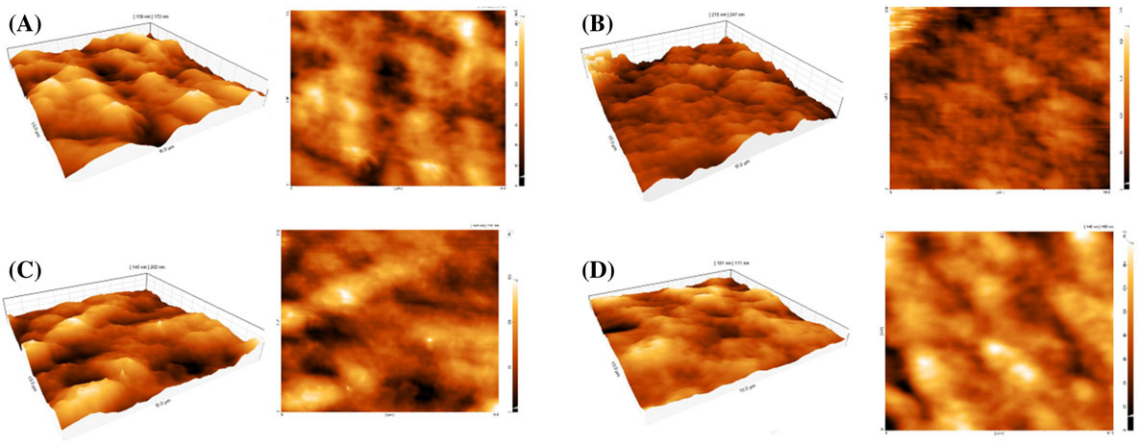

FIGURE 3 AFM images of samples (A) neat TPU, (B) TPU/CBNPs, (C) TPU/HNTs, and (D) TPU/MWCNTs. Nanofiller content = 0.1 wt% [Colour figure can be viewed at wileyonlinelibrary.com]

TABLE 1 Transition temperatures of samples based on the DMTA and DSC analyses

Analysis Sample	DMTA Glass transition temperature of soft segments, °C	DMTA Glass transition temperature of hard segments, °C	DSC	DSC Crystallization temperature, °C	DSC Melting temperature, °C
Neat TPU	−25	110	120	110	190
TPU/MWCNTs (0.1 wt%)	−27	118	128	145	194
TPU/CBNPs (0.1 wt%)	−21	111	120	110	190
TPU/HNTs (0.1 wt%)	−24	113	123	122	192

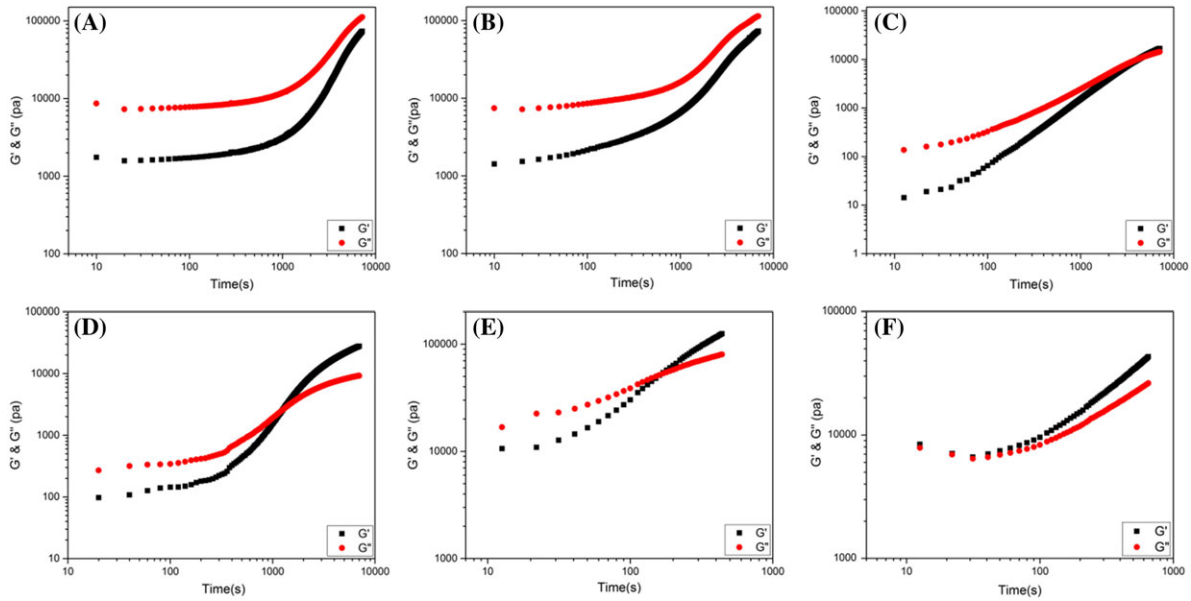

FIGURE 4 Storage and loss moduli of samples as a function of time at 150°C. (A) Neat TPU, (B) TPU/CBNPs, (C) neat TPU applied with preshear rate = 20 s^{-1}, (D) TPU/HNTs, (E) TPU/MWCNTs, and (F) nanocomposite with nanofillers content at upper rheological percolation threshold [Colour figure can be viewed at wileyonlinelibrary.com]

figure, the CBNPs do not change the cross time, whereas the HNTs slightly decrease it. It *is worth mentioning* that the MWCNTs pose the most substantial effect on the cross time and micro-phase separation kinetics. Because both micro-phase separation and crystallization of the PUs are diffusion-controlled processes, the effect of temperature has been fitted with Arrhenius equation. Thermodynamic driving force is able to control the needed time for structuring. This force decreases as the temperature increases. Figure 5 shows cross time as a function of 1/*T* for neat the TPU. This figure corroborates that the experimental points are perfectly fitted with Arrhenius equation:

$$t_{Crosstime} = a.\exp\left(-\frac{b}{T}\right). \quad (1)$$

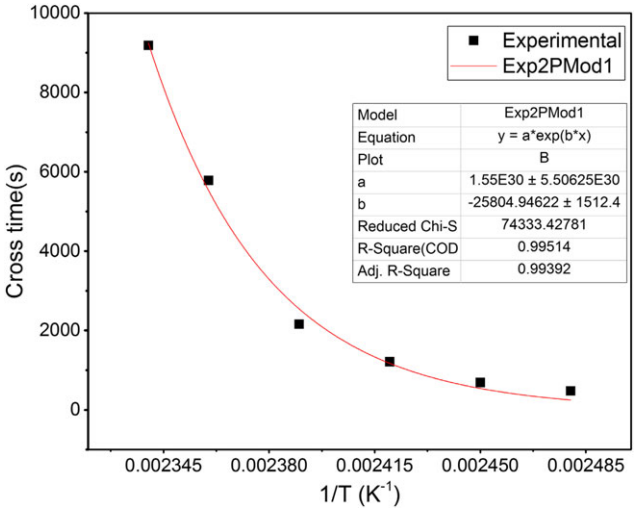

FIGURE 5 Cross time as a function of 1/*T* for neat TPU [Colour figure can be viewed at wileyonlinelibrary.com]

The rheological percolation threshold of MWCNTs is much lower than the conventional fillers, due to their extremely high aspect ratio. Experimental and theoretical approaches have been already used to characterize the factors that govern the rheological percolation threshold of the polymer nanocomposites. Based on some researches, strong correlations between rheological percolation threshold and aspect ratio of the fillers are suggested. For instance, Ren et al revealed a relationship between the rheological percolation threshold and the aspect ratio (A_f)[30] as follows:

$$A_f = 1.5\frac{\phi_{sphere}}{\phi_{percolation}}. \quad (2)$$

Rheological percolation of the interpenetrating, randomly packed spheres happens at φ_{sphere} = 0.29. Li and coworkers showed that the rheological percolation threshold of perfectly dispersed CNTs and agglomerates can be expressed by[31]

$$P_c = \frac{\pi\xi\varepsilon}{6} + \frac{(1-\xi)21.195}{\alpha^2}. \quad (3)$$

In which α is the aspect ratio. **ε** is the local volume fraction of CNT in agglomerate; and **ξ** is the volume fraction of the agglomerated CNTs. **ξ** and **ε** are reliant on the filler dispersion and sample preparation method. In melt mixing process, **ξ** and **ε** should be considered between 0.05 and 0.1. In our calculation, **ξ** and **ε** are assumed equal to 0.05 (Table 2).

As nanofiller content increases, the aspect ratio decreases and solid like behavior emerges. Thus, attempts have been made to modify the formula further matching the experimental data. Because nanofiller aggregation that leads the cross time happens earlier, a modified formula was developed in which the aspect ratio raises with the increase in nanofiller size:

TABLE 2 Theoretical calculation of MWCNTs aspect ratio

MWCNT content, wt%	Aspect ratio based on Equation 2, m^2/g	Aspect ratio based on Equation 3, m^2/g	Aspect ratio based on Equation 4, m^2/g
0.1	450	--	112.5
0.15	300	323	168.75
0.2	225	170.5	225
0.4	112.5	86	450
0.8	56.25	54	900
1.2	37.5	43	1350

$$A_f = 1.5\frac{\phi_{sphere}}{\phi_{percolation}}.\frac{\phi}{\phi_{percolation}}. \quad (4)$$

For different MWCNT content based on Equations 2, 3, and 4, the aspect ratio was calculated, and the data were collected in Table 2. For the MWCNTs, CBNPs, and HNTs at rheological percolation threshold, the aspect ratio was calculated (based on the Equation 2) and compared with experimental data (Table 3). Figure 6 shows the cross time as a function of the MWCNT content at different temperatures. As it can be perceived, with the increase in MWCNT content and decrease in temperature, the cross time occurred earlier. Based on these observations, a theoretical equation was developed as follows:

$$t_{Crosstime} = a.\exp\left(-\frac{b}{T}\right).\frac{20}{A_f}. \quad (5)$$

TABLE 3 Rheological percolation threshold and aspect ratio of nanofillers

Nanofiller	Rheological Percolation Threshold	Aspect Ratio based on Equation 2, m^2/g	Experimental Aspect Ratio, m^2/g
CBNPs	0.05	9	10
HNTs	0.007	64	64
MWNTs	0.002	225	250

This equation has been successfully fitted with the data from Figure 6. It is noteworthy to mention that for neat polymers and nanofillers with aspect ratio less than 20, A_f has been considered as 20. As evidenced from Figure 4C, by applying the shear prior to the time sweep test, due to break of initial structure, there is an initial drop in the storage and loss modulus compared with other samples. However, as time goes on, applied shear enhances the micro-phase separation kinetics. Figure 7 shows the cross time as a function of preshear rate for neat TPU. The results show that the increase in preshear rate decreases the cross time. Based on this data, theoretical equation was developed as follows:

$$t_{Crosstime} = a.\exp\left(-\frac{b}{T}\right) - c.\overset{g}{\dot{\gamma}} \quad (6)$$

where $\overset{g}{\dot{\gamma}}$ is the shear rate. It has to be mentioned that the experimental data offered by Mourier et al[22] have been successfully fitted with this equation. Consequently, this equation could be used for other PU systems or even block copolymers. Finally, considering both neat TPU and the TPU nanocomposites, final equation has been developed:

$$t_{totalCrosstime} = a.\exp\left(-\frac{b}{T}\right).\frac{20}{A_f} - c.\overset{g}{\dot{\gamma}}.\frac{20}{A_f}. \quad (7)$$

According to the experimental findings, effect of the shear rate on micro-phase separation of neat TPU and the CBNPs loaded nanocomposites is more profound than MWCNT and HNT loaded nanocomposites. The advantage of the equation offered here (Equation 7) is that the micro-phase separation time for TPU systems with or without nanofillers at different shear rates and temperatures could be estimated.

Figure 8 schematically illustrates shear induced micro-phase separation of TPU nanocomposites containing MWCNTs. Efforts have been made to depict the MWCNTs and hard segments consistent with the real scale. As evidenced by the figure, by applying shear flow, both hard segments and MWCNTs were oriented. Although hard segments which are away from the MWCNTs are not affected by the MWCNTs,

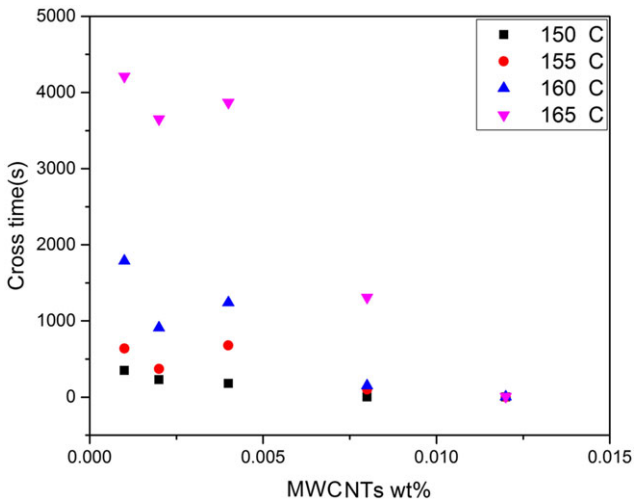

FIGURE 6 Cross time as a function of MWCNTs content at different temperatures [Colour figure can be viewed at wileyonlinelibrary.com]

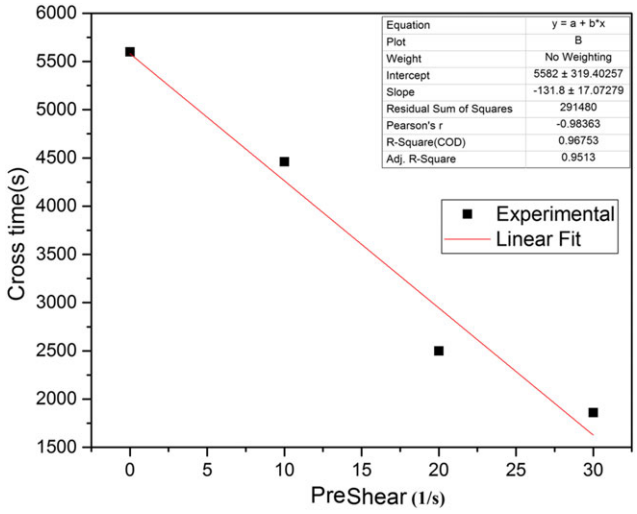

FIGURE 7 Cross time versus preshear rate for neat TPU [Colour figure can be viewed at wileyonlinelibrary.com]

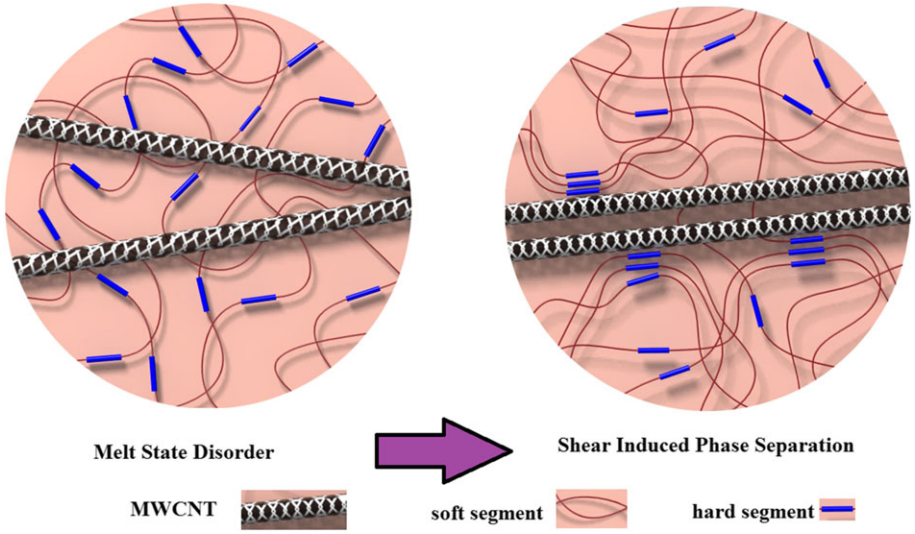

FIGURE 8 Schematic representation for shear induced micro-phase separation of TPU nanocomposite containing MWCNTs [Colour figure can be viewed at wileyonlinelibrary.com]

TABLE 4 Micro-phase separation temperature and crystallization temperature of samples. Nanoparticle content is equal to 0.1 wt%

Sample	Micro-Phase Separation Temperature, °C	Crystallization Temperature, °C
Neat TPU	112	110
TPU/MWNTs	143	145
TPU/HNTs	126	122
TPU/CBNPs	113	110

these tend to be oriented and phase separated due to shear flow. From the Figure 8, it can be concluded that a MWCNT could provide a nucleation site for plenty of the hard segments.

It is well accepted that the rheology is one of the most sensitive tools to study the dynamic of chains and the formation of three-dimensional elastic networks. Hence, to determine the micro-phase separation temperature, temperature sweep test (cooling mode) was used.[32] In the molten state, the loss modulus is higher than the storage one. However, as the temperature decreases, thermodynamic driving force leads to the micro-phase separation. Based on the cooling mode and DSC analyses, micro-phase separation temperature and crystallization temperature of the samples were characterized, and the data were collected in Table 4. Results show that micro-phase separation temperature of the MWCNTs nanocomposite is approximately 31°C higher than that of TPU counterpart due to positive nucleating effect of the MWCNTs. Therefore, by the same logic, the HNTs slightly increase the micro-phase separation temperature and the CBNPs cause no effect. These results are consistent with the DSC data.

4 | CONCLUSION

In the current research, the effect of temperature, shear flow, and nanofillers on micro-phase separation of the TPUs has been studied and formulated. To this end, TPU was synthesized and melt-compounded with three kinds of nanofillers, ie, MWCNTs, Closite 30B nanoplates, and HNTs. Considering dissimilar affinity of the nanofillers to the hard segments, degree of micro-phase separation and properties of nanocomposites would be different. The presence of micro-phase separated domains near the MWCNTs represents the strong affinity of nanofillers to the hard segments; whereas, the CBNPs evidenced no affinity towards the hard segments. *The neat TPU and the nanocomposites undertook time sweep experiments at disparate temperatures, pre-shear and nanofillers*. The findings from these experiments were used to develop an equation expressing influence of temperature, pre-shear and nanofiller aspect ratio on micro-phase separation time of TPU base nanocomposites. Micro-phase separation time of TPU base nanocomposites with or without nanofillers, at different shear rates and temperatures, can be approximated by the proposed equation. The equation could be used to estimate micro-phase separation time of other PU systems or even block copolymers.

ORCID

Vahid Haddadi-Asl http://orcid.org/0000-0002-2728-6307

REFERENCES

1. Akindoyo JO, Beg M, Ghazali S, Islam M, Jeyaratnam N, Yuvaraj A. Polyurethane types, synthesis and applications—a review. *RSC Adv*. 2016;6(115):114453-114482.
2. Sahebi Jouibari I, Haddadi-Asl V, Mirhosseini MM. Effect of nanofiller content and confined crystallization on the microphase separation kinetics of polyurethane nanocomposites. *Polym Compos*.
3. Zajac M, Kahl H, Schade B, Rödel T, Dionisio M, Beiner M. Relaxation behavior of polyurethane networks with different composition and crosslinking density. *Polymer*. 2017;111:83-90.
4. Noreen A, Zia KM, Zuber M, Tabasum S, Zahoor AF. Bio-based polyurethane: an efficient and environment friendly coating systems: a review. *Prog Org Coat*. 2016;91:25-32.
5. Sinturel C, Bates FS, Hillmyer MA. *High χ-low N block polymers: how far can we go?* ACS Publications; 2015.

6. Velankar S, Cooper SL. Microphase separation and rheological properties of polyurethane melts. 1. Effect of block length. *Macromolecules*. 1998;31(26):9181-9192.
7. Leung LM, Koberstein JT. DSC annealing study of microphase separation and multiple endothermic behavior in polyether-based polyurethane block copolymers. *Macromolecules*. 1986;19(3):706-713.
8. Han CD, Kim J, Kim JK. Determination of the order-disorder transition temperature of block copolymers. *Macromolecules*. 1989;22(1):383-394.
9. Han CD, Baek DM, Kim JK. Effect of microdomain structure on the order-disorder transition temperature of polystyrene-block-polyisoprene-block-polystyrene copolymers. *Macromolecules*. 1990;23(2):561-570.
10. He Y, Xie D, Zhang X. The structure, microphase-separated morphology, and property of polyurethanes and polyureas. *J Mater Sci*. 2014;49(21):7339-7352.
11. Velankar S, Cooper SL. Microphase separation and rheological properties of polyurethane melts. 3. Effect of block incompatibility on the viscoelastic properties. *Macromolecules*. 2000;33(2):395-403.
12. Chuang W-T, Jeng U-S, Sheu H-S, Hong P-D. Competition between phase separation and crystallization in a PCL/PEG polymer blend captured by synchronized SAXS, WAXS, and DSC. *Macromol Res*. 2006;14(1):45-51.
13. Laxminarayan A, McGuire KS, Kim SS, Lloyd DR. Effect of initial composition, phase separation temperature and polymer crystallization on the formation of microcellular structures via thermally induced phase separation. *Polymer*. 1994;35(14):3060-3068.
14. Finnigan B, Martin D, Halley P, Truss R, Campbell K. Morphology and properties of thermoplastic polyurethane composites incorporating hydrophobic layered silicates. *J Appl Polym Sci*. 2005;97(1):300-309.
15. Landa M, Canales J, Fernández M, Muñoz ME, Santamaría A. Effect of MWCNTs and graphene on the crystallization of polyurethane based nanocomposites, analyzed via calorimetry, rheology and AFM microscopy. *Polym Test*. 2014;35:101-108.
16. Mirhosseini MM, Haddadi-Asl V, Zargarian SS. Fabrication and characterization of polymer-ceramic nanocomposites containing pluronic F127 immobilized on hydroxyapatite nanoparticles. *RSC Adv*. 2016;6(84):80564-80575.
17. Barick AK, Tripathy DK. Preparation, characterization and properties of acid functionalized multi-walled carbon nanotube reinforced thermoplastic polyurethane nanocomposites. *Mater Sci Eng, B*. 2011;176(18):1435-1447.
18. Gupta Y, Bhave T, Chakraborty A, Pandey A, Sharma R, Setua D. Nonisothermal crystallization kinetics of carbon nanotubes containing segmented polyurethane elastomer. *Polym Eng Sci*. 2016;56(11):1248-1258.
19. Song M, Xia H, Yao K, Hourston D. A study on phase morphology and surface properties of polyurethane/organoclay nanocomposite. *Eur Polym J*. 2005;41(2):259-266.
20. Horst R, Wolf B. Calculation of shear influences on the phase separation behavior of polymer solutions in the region of their lower critical solution temperature. Creation of closed miscibility gaps. *Macromolecules*. 1991;24(9):2236-2239.
21. Mourier E, David L, Alcouffe P, Rochas C, Méchin F, Fulchiron R. Composition effects of thermoplastic segmented polyurethanes on their nanostructuring kinetics with or without preshear. *J Polym Sci B*. 2011;49(11):801-811.
22. Mourier E, Fulchiron R, Méchin F. Shear-induced structuring kinetics in thermoplastic segmented polyurethanes monitored by rheological tools. *J Polym Sci B*. 2010;48(2):190-201.
23. D'Haese M, Van Puyvelde P, Langouche F. Effect of particles on the flow-induced crystallization of polypropylene at processing speeds. *Macromolecules*. 2010;43(6):2933-2941.
24. Garcia-Gutierrez M, Hernandez J, Nogales A, Panine P, Rueda D, Ezquerra T. Influence of shear on the templated crystallization of poly (butylene terephthalate)/single wall carbon nanotube nanocomposites. *Macromolecules*. 2008;41(3):844-851.
25. Pedrazzoli D, Manas-Zloczower I. Understanding phase separation and morphology in thermoplastic polyurethanes nanocomposites. *Polymer*. 2016;90:256-263.
26. Zhang X, Xu R, Wu Z, Zhou C. The synthesis and characterization of polyurethane/clay nanocomposites. *Polym Int*. 2003;52(5):790-794.
27. Unalan IU, Cerri G, Marcuzzo E, Cozzolino CA, Farris S. Nanocomposite films and coatings using inorganic nanobuilding blocks (NBB): current applications and future opportunities in the food packaging sector. *RSC Adv*. 2014;4(56):29393-29428.
28. Fernández-d'Arlas B, Khan U, Rueda L, et al. Influence of hard segment content and nature on polyurethane/multiwalled carbon nanotube composites. *Compos Sci Technol*. 2011;71(8):1030-1038.
29. Yoon PJ, Han CD. Effect of thermal history on the rheological behavior of thermoplastic polyurethanes. *Macromolecules*. 2000;33(6):2171-2183.
30. Ren J, Silva AS, Krishnamoorti R. Linear viscoelasticity of disordered polystyrene-polyisoprene block copolymer based layered-silicate nanocomposites. *Macromolecules*. 2000;33(10):3739-3746.
31. Li, J., Ma, P., Sze, C., Kai, T., Tang, B., and Kim, J. K. Percolation threshold of polymer nanocomposites containing graphite nanoplatelets and carbon nanotubes, In *ICCM International Conferences on Composite Materials*.(2007)
32. Nichetti D, Grizzuti N. Determination of the phase transition behavior of thermoplastic polyurethanes from coupled rheology/DSC measurements. *Polym Eng Sci*. 2004;44(8):1514-1521.

How to cite this article: Sahebi Jouibari I, Haddadi-Asl V, Mirhosseini MM. Formulation of micro-phase separation kinetics of polyurethane nanocomposites. *Polym Adv Technol*. 2018;1–8. https://doi.org/10.1002/pat.4410